New insights on waste mixing for enhanced fermentative hydrogen production

Lucie Perat, Renaud Escudié, Nicolas Bernet, Charlotte Richard, Mathilde Jégoux, Marine Juge, Eric Trably

Process Safety and Environmental Protection 188 (2024) 1326–1337

Contents lists available at ScienceDirect

Process Safety and Environmental Protection

journal homepage: www.journals.elsevier.com/process-safety-and-environmental-protection

New insights on waste mixing for enhanced fermentative hydrogen production

Lucie Perat [a], Renaud Escudié [a], Nicolas Bernet [a], Charlotte Richard [b], Mathilde Jégoux [b], Marine Juge [b], Eric Trably [a,*]

[a] INRAE, Univ Montpellier, LBE, 102 avenue des Étangs, Narbonne 11100, France
[b] ENGIE Lab CRIGEN, 4 rue Joséphine Baker, Stains 93240, France

ARTICLE INFO

Keywords:
Biohydrogen
Carbohydrate content
Dark-fermentation
Microbial community
Waste
Co-fermentation

ABSTRACT

Co-fermentation can differently impact H_2 production, with positive or negative interactions observed. Positive interactions were usually attributed to a balanced composition and improved buffer capacity. However, the impact of co-fermentation on microbial communities (H_2-producing and H_2-consuming bacteria) remains unexplored. This work aimed to deepen the interaction mechanisms observed in co-fermentation targeting microbial communities with an innovative focus on H_2-consuming bacteria (homoacetogens). The H_2 production of seven mixtures (food waste fractions and rye silage) and individual performances were compared by Biochemical Hydrogen Potential (BHP). Final microbial communities were characterized by sequencing and qPCR. A positive correlation between H_2 yield and Soluble and Easily Extractible Sugars (SEES) content was observed for all the substrates ($R^2 = 0.79$), confirming this correlation not only for individual substrates but also mixtures. Positive interactions were observed for most of the mixtures, with a H_2 yield significantly higher (16–37 %) than expected. The faster H_2 production observed in mixtures (2.6 times faster) was correlated to the selection of *Clostridiaceae_1* family (final relative abundance of 90–98 %) and decline of homoacetogens. It is therefore essential to further understand the microbial communities' dynamics in co-fermentation to develop efficient fermentation systems.

1. Introduction

In 2020, 80 % of the hydrogen produced worldwide was derived from fossil fuels, resulting in 900 Mt of CO_2 emissions (International Energy Agency, 2021). The use of H_2 as an alternative to fossil fuels necessitates first to massively decarbonize its production with cleaner and renewable processes. According to Dincer and Acar (2015), biological processes have the least harmful impacts on the environment compared to fossil fuel-based or nuclear-based processes (Dincer and Acar, 2015). Among these biological processes, Dark Fermentation (DF) appears as one of the most promising technologies for biological H_2 ($bioH_2$) production, while treating and valorizing organic waste (Ghimire et al., 2015). However, DF presents low conversion yields mainly due to inhibitions and H_2-consuming bacteria in mixed cultures (Bundhoo and Mohee, 2016). Remaining organic matter in DF effluent can be further valorized by coupling DF with other processes such as Anaerobic Digestion (AD) leading to an improved energetic yield (Cremonez et al., 2021). Coupling DF with AD is however a challenge at higher scale as most of the waste streams valorized in AD are complex residues with a varying composition that could not be compatible with H_2 production. Indeed, in DF, waste composition (carbohydrates, lipids, proteins) greatly influences H_2 production and stability (Alibardi and Cossu, 2015). The highest H_2 yields in the literature were reached for carbohydrate-rich waste. (Okamoto et al., 2000; Lay et al., 2003). In contrast, lipid-rich substrates and protein-rich substrates are not favorable for H_2 production. Lipids-rich substrates perform low H_2 yield due to thermodynamic limitation (Dong et al., 2009) and the release of Long Chain Fatty Acids (LCFA) during lipids hydrolysis inhibiting anaerobic

Abbreviations: BHP, Biochemical Hydrogen Potential; $BioH_2$, Biological Hydrogen; BSA, Bovine Serum Albumine; C/N, Carbon to Nitrogen ratio; COD, Chemical Oxygen Demand; DF, Dark Fermentation; H_2, Hydrogen; HPB, Hydrogen-Producing Bacteria; HPE, Hydrogen Production Efficiency; LAB, Lactic Acid Bacteria; LCFA, Long Chain Fatty Acids; N_2, Nitrogen; PCoA, Principal Coordinate Analysis; S/X, Substrate to Inoculum ratio; SEES, Soluble and Easily Extractible Sugars; TKN, Total Kjeldahl Nitrogen; TS, Total Solids; VS, Volatile Solids.

* Corresponding author.
E-mail address: eric.trably@inrae.fr (E. Trably).

https://doi.org/10.1016/j.psep.2024.06.006
Received 27 February 2024; Received in revised form 13 May 2024; Accepted 2 June 2024
Available online 3 June 2024

bacteria (Henderson, 1973; Hanaki et al., 1981). Concerning protein-rich substrates, the Stickland reaction (major amino acid degradation pathway) does not produce H_2 and the release of ammonium during protein hydrolysis can be inhibitory above threshold levels (Chen et al., 2021). Yet, synthetic proteins and lipids (hydrolyzed casein and virgin olive oil) had an indirect positive impact on H_2 pathways when present in optimized proportions in mixtures with glucose (Tarazona et al., 2022). Therefore, as most organic waste streams contain not only carbohydrates but also lipids and proteins (Alibardi and Cossu, 2015), we need to better understand the impacts of lipids-protein-carbohydrates mixture on DF performances. This will help for waste management optimization and DF-AD coupling.

Several studies worked with mixtures of substrates, so-called co-fermentations (in contrast to co-digestion for methane production), and observed an enhanced H_2 production. The improved H_2 production observed in co-fermentation studies was related to synergetic effects (positive interactions) usually attributed to: i) improved buffer capacity, ii) balance of composition and nutrients, iii) dilution of toxic compounds and iv) appropriate C/N ratio (Boni et al., 2013; Xue et al., 2020; Policastro et al., 2022). Positive interactions were defined when the co-fermentation yield is higher than the expected one *i.e.*, the weighted sum of the mono-fermentation yield of the mixture components (Yang and Wang, 2017). However, synergy is not always observed as the nature of interactions in mixtures seems to depend on the mixing ratio, substrate type and operational conditions. Indeed, several co-fermentations studies of sewage sludge with different organic waste such as fallen leaves (Yang et al., 2019) or flower waste (Yang and Wang, 2018) favored positive synergetic interactions. In contrast, Yilmazel and Duran (2021) observed antagonist interactions in pure culture with mixture of cattle manure, wastewater bio-solids and switch grass, with experimental H_2 production 15–30 % lower than expected (Yilmazel and Duran, 2021). Alibardi and Cossu (2016) observed both positive and negative interactions for co-fermentation of food waste fractions. The authors attributed these gaps (ranging from - 8–17 %) more to the sum of experimental errors rather than interaction effects (Alibardi and Cossu, 2016).

Yang and Wang (2021) considered that most of co-fermentation studies focused on production performances related to waste composition with little consideration to microbial communities (Yang and Wang, 2021). The identification of microbial communities is however a key step to better understand the microbial process of dark co-fermentation and optimize it (Gomez-Romero et al., 2014). The understanding of interaction mechanisms in co-fermentation could therefore be deepened, with a specific focus at the microbial level. Indeed, Wang et al. (2013) showed that the microbial communities were impacted in co-fermentation conditions, even when small amounts of co-substrates were added to cassava stillage: *Clostridium cellulosi* specifically grown in co-fermentation conditions contrary to the individual cassava stillage fermentation (Wang et al., 2013). Nonetheless, to the authors' knowledge no information is available concerning the impact of co-fermentation on both hydrogen-producing bacteria and homoacetogenic bacterial activity, the latter being known to consume H_2 and CO_2 and reduce the H_2 yield (Wang and Yin, 2019). The aim of this work was therefore to deepen the interaction mechanisms observed in co-fermentation with a specific focus on microbial communities. Here, the H_2 production of eight substrates both individually and in seven different mixtures were compared to identify the potential interactions between macro-composition (carbohydrates, lipids, proteins) of the substrates and the emergence of microbial communities (H_2-producing or H_2-consuming bacteria). The novelty of this study relies on the number of substrates co-fermented, closer to the real composition of complex waste stream, as well as the objective to investigate the impact of co-fermentation on microbial communities and homoacetogenesis. (Fig. 1)

2. Materials and methods

2.1. Inoculum preparation

The microbial inoculum corresponded to a fresh aerobic sludge collected at the wastewater treatment plant of Narbonne, France. According to Chatellard's work, this fresh sludge showed an interesting H_2 yield on glucose (129 $mL_{H2}/g_{initialCOD}$) (Chatellard, 2016). After sampling, the fresh sludge was immediately centrifuged (10 min at 16.800 g). The pellet was subsequently freeze-dried, grinded, and stored at - 80 °C. It was shown that storing the sludge in freeze-dried condition did not impact H_2 performances and microbial communities for storage period of 1.5 months (Dauptain et al., 2021). Total Solids (TS) and Volatile Solids (VS) were then determined according to standard methods (Magdalena et al., 2023). The VS/TS ratio was constant and of 0.97. Before use, an aliquot was defrosted, diluted in 200 mL of ultrapure water and heat-treated. Thermal pre-treatment at 90 °C for 15 min was then applied using a hot plate (CMAG H57, IKA, Germany, Staufen) coupled with a temperature probe (ETS D5, IKA, Staufen, Germany) to select spore-forming bacteria over methanogenic archaea. Non-sporulating methanogenic archaea were efficiently removed as no

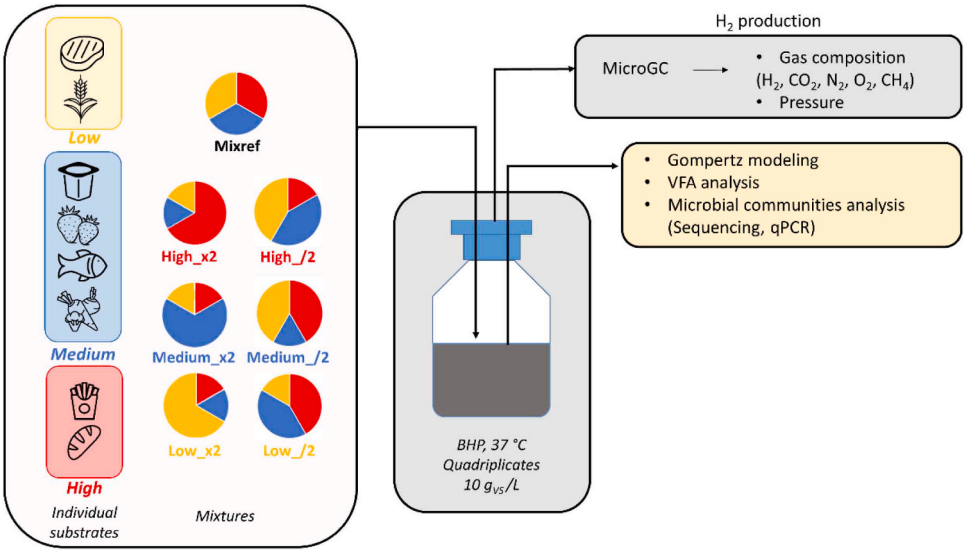

Fig 1. Schematic of the experimental process. 1-column fitting image.

methane production was detected for all the conditions tested.

2.2. Substrates preparation

The aim of this study was to assess the impact of mixture composition on dark fermentation performances. Several substrates were studied individually, and mixed in different proportions. The substrates used in this study were inspired from the French average composition of food waste, as detailed in Dauptain et al., (2020). The ingredients of the food waste recipe described by Dauptain et al., (2020) were studied individually and corresponded to the following food waste fractions: steak, yogurt, red berries, breaded fish, French fries, bread and vegetables. Each food waste fraction was purchased at the supermarket and stored separately at – 20 °C. Rye silage was also included in this study, as an individual substrate and in the mixtures' compositions. Completing food waste fractions with rye silage allowed to reach a raw composition closer to the industrial waste stream treated by waste valorization units, as in 2021 in France energy crop covers accounted for 33 % of the organic matter valorized by anaerobic digestion units (ADEME, 2021, in French). Rye was initially grown as an energy cover crop and silage conditions were applied for storage. After delivery, rye silage was stored at – 20 °C. Before their use as substrates, the synthetic waste or their mixtures were grinded and diluted to reach 10 % TS. Synthetic food waste from animal source (steak, breaded fish, yogurt) were considered as animal by-product to be valorized. To comply with the EU Regulation No 142/2011 defining the uses and valorization of animal by-products not intended for human consumption, a thermal pre-treatment (hygienization) was applied (Official Journal of the European Union, 2011). This pretreatment was defined by the EU regulation and consisted in heating for 1 h at 70 °C using water bath. It was performed for all the substrates for consistency. After this hygienization step, the diluted waste was sieved (2 mm mesh).

2.3. Mixture compositions

Food waste and rye silage were firstly mixed and defined as reference mixture (Mixref). The composition of Mixref was inspired by the synthetic food waste used by Dauptain et al., (2020) complemented with 20 % (wet percentage) of rye silage. The H_2 production of each individual component of the Mixref was first assessed to classify them according to their DF performances: "High" group, was determined when yields exceeded 130 mLH_2/g_{VS}, "Medium" group for yields ranging between 40 and 110 mL_{H2}/g_{VS} and "Low" group corresponded to substrates showing yields lower than 10 mL_{H2}/g_{VS}. The composition of Mixref was then modified to understand the impact of specific components within the mixture. The raw percentage of each group was then doubled or halved, resulting in six new mixtures ("High_x2", "High_/2", "Medium_x2", "Medium_/2", "Low_x2", "Low_/2"). The proportions of components in the other groups were kept constant and balanced in relation to Mixref composition. The details of the substrate compositions, on a wet basis, for the 7 mixtures are presented in Table 1 while the composition in VS basis is available in supplementary file S1. A schematic rig is presented in Figure 1.

*Med is abbreviation for "Medium"

2.4. Composition of substrates

The composition in carbohydrates, proteins and lipids of both individual and mixed substrates was analyzed. Carbohydrates content was measured following the protocol of Guo et al. (2014). This involved an initial step of mild hydrolysis to extract carbohydrates where 0.5 g of substrate was mixed with 40 mL of 2 M Hydrochloric acid (HCl) for 1 h in an ultrasonic bath. After hydrolysis, carbohydrate concentration was measured in quadruplicate using the anthrone method, using glucose as standard. Results were expressed in mg of glucose equivalent per gram of volatile solids.

For this study, the measurements were performed on the diluted substrates after hygienization, rather than on raw freeze-dried samples as done by Guo et al. (2014), to ensure a composition of the substrate similar to what was present in the BHP bottles. The carbohydrate content measured here corresponded to Soluble and Easily Extractible Sugars (SEES). The protein content was estimated using Total Kjeldahl Nitrogen (TKN) method in triplicate (Charnier et al., 2017). The grams of nitrogen were then converted into grams of proteins using conversion ratios related to substrate nature, as reviewed by Mariotti et al., (2008). Lipids were analyzed by Soxhlet extraction method (INNOLAB, Troyes, France).

The C/N ratio was determined for each individual substrate by CHNS analysis (Flash SMART, Thermo Fisher SCIENTIFIC). The C/N ratio of the mixtures of substrates were calculated based on the results obtained on each individual substrate.

The composition of the substrates (after hygienization and sieving),

Table 2
Substrate macro-molecular composition (SEES, proteins and lipids) for the individual substrates and mixtures. Composition measured on the diluted and hygienised substrates.

Substrates	SEES* (mg/g_{VS})	Proteins (mg/g_{VS})	Lipids (mg/g_{VS})	C/N
Steak	9.85 ± 1.66	474.72 ± 87.02	394.11 ± 13.56	7.04
Rye silage	160.54 ± 56.58	76.38 ± 0.13	14.53 ± 0.50	30.11
Yogurt	231.55 ± 11.67	307.58 ± 11.87	105.54 ± 3.63	10.33
Red berries	591.18 ± 28.75	82.04 ± 5.15	2.20 ± 0.08	36.42
Breaded fish	700.54 ± 47.79	321.39 ± 26.33	93.51 ± 3.22	11.28
Vegetables	1073.28 ± 167.60	75.04 ± 14.19	144.77 ± 4.98	34.99
French fries	819.88 ± 51.73	61.06 ± 9.34	133.66 ± 4.60	33.21
Bread	949.34 ± 88.21	152.21 ± 3.46	10.49 ± 0.36	22.89
Mixref	604.76 ± 48.99	198.44 ± 3.12	97.99 ± 7.97	17.00
Low_x2	369.75 ± 47.62	252.98 ± 6.12	129.45 ± 10.52	14.40
Low_/2	691.11 ± 43.18	166.05 ± 5.94	92.04 ± 7.48	18.76
Medium_x2	531.93 ± 46.02	198.26 ± 19.54	97.38 ± 7.92	17.85
Medium_/2	589.60 ± 83.78	212.13 ± 34.96	96.19 ± 7.82	16.59
High_x2	682.73 ± 45.48	159.80 ± 3.92	74.93 ± 6.09	19.77
High_/2	498.73 ± 56.33	240.66 ± 10.60	123.48 ± 10.04	15.96

* Sugars concentration correspond to Soluble and Easily Extractible Sugars (SEES) but not total sugars. The concentration is expressed in mg of glucose equivalent

Table 1
Raw composition in wet percentage of food waste and rye silage for the mixtures studied.

Component	Mixref	High_x2	High_/2	Med_x2*	Med_/2*	Low_x2	Low_/2
Steak	12	7.33	14.33	4	16	24	6
Rye silage	20	12.22	23.89	6.67	26.67	40	10
Yogurt	8	4.89	9.56	16	4	4.24	9.88
Red berries	12	7.33	14.33	24	6	6.35	14.82
Breaded fish	8	4.89	9.56	16	4	4.24	9.88
Vegetables	12	7.33	14.33	24	6	6.35	14.82
French fries	16	32	8	5.33	21.33	8.47	19.76
Bread	12	24	6	4	16	6.35	14.82

including SEES, proteins and lipids is presented in Table 2.

2.5. Hydrogen production measurement

Hydrogen production was assessed by BHP tests, for each substrate in quadruplicate. BHP tests aim to determine the maximal cumulated volume of H_2 produced for a given substrate. The BHPs were carried out in 600 mL bottles with a working volume of 200 mL, under mesophilic conditions (37 °C) in batch. The substrate concentration was set at 10 g_{VS}/L and the Substrate to Inoculum ratio (S/X) at 20 g_{VS} /g_{VS}. The culture medium consisted of 100 mol/L of 2-(N-morpholino)ethanesulfonic acid (MES buffer), 0.5 g/L of K_2HPO_4 and 1 mL of a micronutrient solution (composition detailed in Noguer et al., (2022). The heat-treated substrate and inoculum were added to the bottles and the working volume was adjusted with osmosed water. The initial pH was adjusted at 6 using NaOH 8 M and HCl 25 % (w/w). The bottles were sealed using butyl-rubber stoppers and aluminum caps, and the headspace was flushed with nitrogen (N_2) to ensure anaerobic conditions.

Gas composition (H_2, CO_2, O_2, N_2, CH_4) was monitored every two hours during fermentation and pressure was adjusted using a micro-gas chromatograph (microGC) (SRA l-GC R3000) as described by Ben Yahmed et al., (2021). BHP experiments were stopped when H_2 production reached a plateau (stable total H_2 production).

The kinetic parameters of H_2 production was modelled overtime using the modified Gompertz model (Eq. 1). Modeling was carried out using RStudio with the grofit package developed by Kahm et al. (2010). Hydrogen yield was expressed as the ratio between the final cumulative H_2 volume (mL) and the initial quantity of VS of substrate.

$$H(t) = H_{\max}\exp\left(-\exp\left(\frac{R.e}{H_{\max}}(\lambda - t) + 1\right)\right) \quad (1)$$

Where Hmax is the maximal quantity of H_2 produced (mLH_2/g_{VS}), R is the maximal rate of H_2 production (mLH_2/g_{VS}/d) and λ the lag phase (d)

Two mL of liquid samples were sampled in duplicate from each BHP replicate at start and at the end of the fermentation tests. The samples were centrifuged for 15 min at 13,000 g using an Eppendorf Minispin centrifuge. The supernatants and pellets were stored at - 20 °C for further analysis.

The Hydrogen Production Efficiency (HPE) was calculated based on the following equation (Eq2). This ratio is used to compare the experimental H_2 produced with the theoretical one, estimated on the acetate and butyrate production on a molar basis as presented by Arooj et al. (2008) and Luo et al. (2011). It assesses the extent to which acetate production is associated with homoacetogenesis or related to H_2 production.

$$HPE = \frac{H_{2experiment}}{2(Acetate + Butyrate)} \quad (2)$$

2.6. Analytical measurements

Supernatants were filtered at 0.2 µm (nylon filter) before analyses. Volatile Fatty Acids (VFA), *i.e.* acetate, propionate, butyrate, isobutyrate, valerate and isovalerate were analyzed by Gas Chromatography (GC). The device was a Clarus 580 gas chromatograph (Perkin Elmer) with an Alltech-FFAP EC™1000 column and Flame Ionization Detector (FID) using N_2 as gas carrier (flow of 6 mL/min) (Noguer et al., 2022). Ethanol and organic acid concentrations (lactic acid, succinic acid) were measured with High Performance Liquid Chromatography (HPLC). The HPLC was composed of a HPX-87 H column (300 × 7.8 mm, Biorad) equipped with a protective precolumn (Microguard cation H refill catbridges, Biorad) (Dauptain et al., 2020). The column temperature was set at 35 °C and ran with 4 mM H_2SO_4 solution as eluent and flow rate of 0.3 mL/min. The detector was a refractive index detector, set at 45 °C (Dauptain et al., 2020).

2.7. Microbial community analyses

Two different analytical techniques were used in this study to characterize microbial communities. Illumina Miseq sequencing was used to determine the relative abundance of microbial communities. On the other hand, quantitative PCR (qPCR) was assessed to quantify bacteria members (total bacteria), hydrogen-producing bacteria and homoacetogenic bacteria.

For each substrate, one sample was collected at start of the fermentation test (t0) and duplicate at the end of fermentation (tf) for microbial community analyses. The samples to be analyzed were selected to represent the average H_2 production of a given substrate (individual and mixed substrates). DNA was extracted from the pellets of liquid samples with a FastDNA™ SPIN kit (MP biomedicals) following the manufacturer's instructions.

For sequencing analysis, the V3-V4 region of the 16 S rRNA gene was firstly amplified to identify bacterial members, as presented by Braga Nan et al. (2020). For this study, the PCR mix contained iProof™ High-Fidelity DNA Polymerase (Bio-Rad laboratories, Inc.) (0.02 u/µL) with its enzyme buffer, forward and reverse primers (0.5 mM), dNTP (0.2 mM), sample DNA (0.04–0.2 ng/µL) and water for a final volume of 60 µL. The PCR amplification program was as reported by Braga Nan et al. (2020). Illumina Miseq sequencing was carried out by the GeT-Biopuces platform (TBI, INSA Toulouse). Mothur version 1.48.0 was used for reads cleaning, assembly and quality checking. Alignment and taxonomic outline were performed using SILVA 132. Sequences were grouped into Operational Taxonomic Units (OTUs) with 97 % similarity. Sequences were submitted to Bioproject MELINBIOH N° PRJNA990529.

qPCR was carried out to quantify total bacteria, hydrogen-producing bacteria and homoacetogens, using SsoAdvanced™ Universal SYBR® Green Supermix. For total bacteria quantification, the V3 region of the 16 S rRNA gene was amplified using primers W49 and W31 as described by Wéry et al. (2008). The PCR program was the following: 2 min at 95 °C, 40 cycles at 95 °C for 10 s and 61 °C for 20 s. For homoacetogenic bacteria quantification, the *formyltetrahydrofolate synthetase* (FTHFS) gene was targeted using primers, PCR mix and program described by Braga Nan et al. (2020). Hydrogen-producing bacteria were quantified by targeting the *hydA* gene as presented by Quéméneur et al. (2011). The qPCR mix was modified as follow: 6 µL of Sybr Green, 1 µL of each primer (250 nM), 2 µL of DNA and 2 µL of water for a total volume of 12 µL. The PCR program was the following: enzyme activation at 95 °C for 2 minutes, 40 cycles at 95 °C for 15 s and 60 °C for 30 s, followed by a melting curve.

2.8. Statistical analyses

All statistical analyses were performed using R software. Statistical comparisons between expected and experimental values were assessed using one sample t-test, using the expected values as reference. Normal distribution was checked using the Shapiro test. When normal distribution hypothesis was not respected, Wilcoxon test was used instead of t-test. The Dunnett test (function DunnettTest from DescTools package) was used to compare the modified mixtures with the control reference (Mixref).

Principal Coordinate Analysis (PCoA) was performed using the capscale function from vegan package (Oksanen et al., 2012) with Bray-Curtis dissimilarity matrix applied at the family level (subset of the sequencing data using aggregate_top_taxa2 from microbiomeutilities package (Shetty and Lahti, 2022)). Families abundances were added to the ordination plot (bold blue arrows) following the approach implemented for the biplot.pcoa function (ape package [37]), using the scaled covariance matrix between families abundances and eigenvectors (Paradis et al., 2004). Environmental variables were fitted to the ordination using the envfit function from the vegan package (Oksanen et al., 2012).

3. Results and discussion

3.1. Correlation between hydrogen yields of individual substrates and mixtures and their content in Soluble and Easily Extractible Sugars (SEES)

BHP tests were conducted for individual substrates and mixtures. For all the conditions investigated, no CH_4 production was observed, confirming the efficiency of the thermal pretreatment to inactivate methanogens. Fig. 2-A presents the average H_2 yield for all individual substrates. Bread achieved the highest H_2 yield, with a value of 184.63 ± 10.64 mLH_2/g_{VS}, followed by French fries (137.65 ± 22.89 mLH_2/g_{VS}), vegetables (101.14 ± 1.62 mLH_2/g_{VS}), breaded fish (67.72 ± 6.95 mLH_2/g_{VS}), red berries (62.15 ± 9.75 mLH_2/g_{VS}), yogurt (49.77 ± 8.45 mLH_2/g_{VS}) and rye silage (9.69 ± 1.68 mLH_2/g_{VS}). The lowest H_2 yield was measured for steak with only 4.25 ± 2.37 mLH_2/g_{VS}.

The individual substrates were grouped on the basis of the H_2 yields: the "High" class included bread and French fries (yield exceeding 130 mLH_2/g_{VS}), the "Medium" class grouped intermediate substrates (yogurt, red berries, breaded fish, vegetables) with a H_2 yield ranging from 40 to 110 mLH_2/g_{VS}, and the "Low" class was composed of steak and rye silage presenting H_2 yields below 10 mLH_2/g_{VS}.

Based on this classification, the composition of Mixref was modified either by doubling or halving the raw percentage of a particular class, resulting in six different modified mixtures (Table 1). The impact of the composition was assessed by comparing the H_2 yield of Mixref with the six new conditions using the Dunnett test, and considering Mixref as the reference. The H_2 yield (in mLH_2/g_{VS}) of Mixref and the six mixtures are presented in Fig. 2-B. Significant differences between Mixref and low class mixtures (Low_x2 and Low_/2) were observed, with a decrease of the H_2 yield from 100.37 ± 11.73 mLH_2/g_{VS} to 55.86 ± 2.46 mLH_2/g_{VS} (p-value = 4.22×10^{-9}) for Low_x2, while Low_/2 increased H_2 yield up to 134.78 mLH_2/g_{VS} (p-value = 3.34×10^{-5}). Interestingly, High_x2 presented a similar yield (135.93 mLH_2/g_{VS}) to Low_/2, with a significant increase compared to Mixref (p-value = 2.5×10^{-6}).

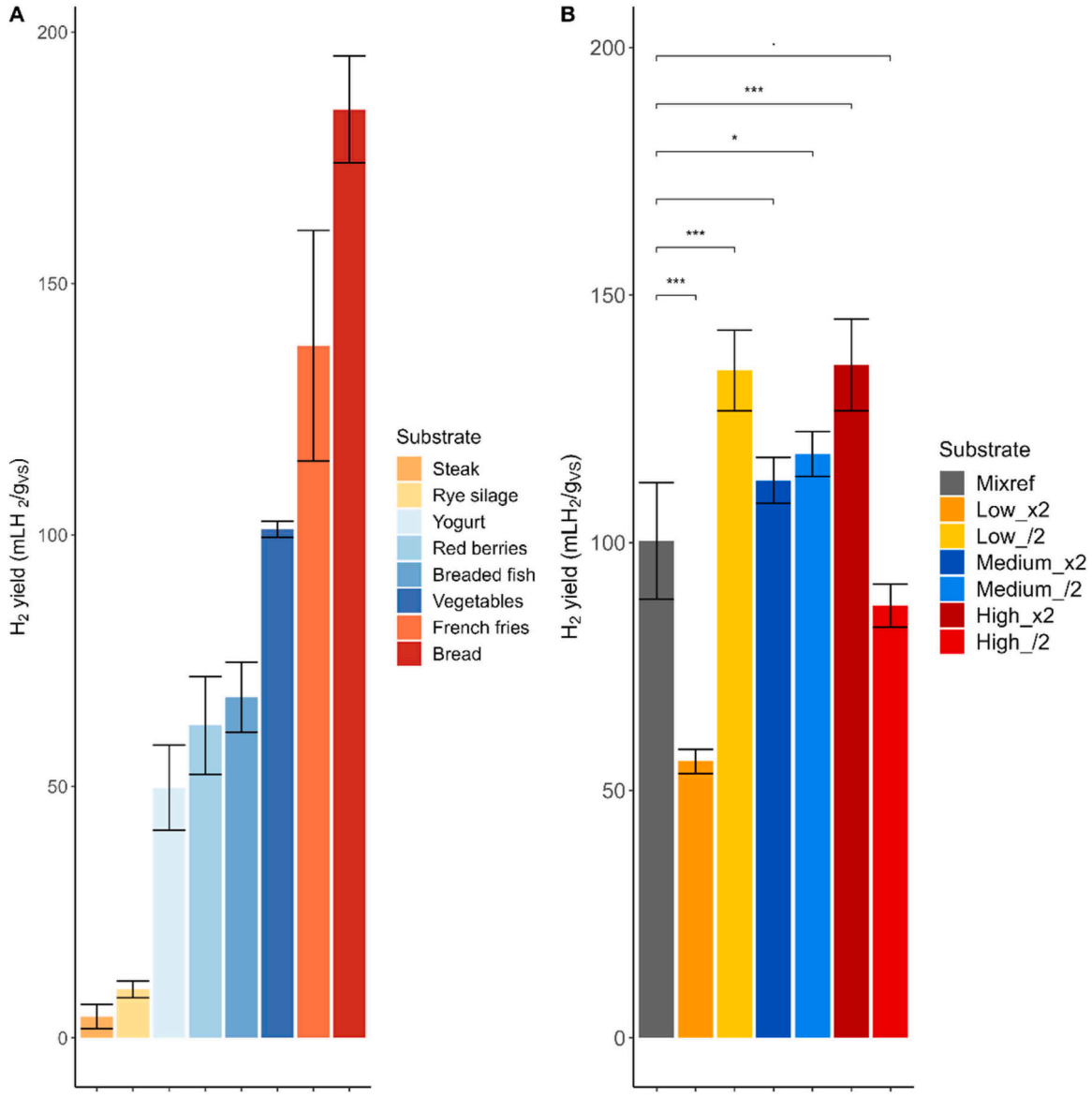

Fig. 2. H_2 yields for individual substrates (2-A) and mixtures (2-B). Fig. 2-A: Mean H_2 yield and standard deviation for individual substrates, classified according to their individual yield: "High class" (red color) for yields superior to 130 mLH_2/g_{VS}; "Medium class" (blue color) for yields between 40 and 110 mLH_2/g_{VS}; "Low class" (yellow color) for yields below 10 mLH_2/g_{VS}. Fig. 2-B: Mean H_2 yield and standard deviation for mixtures: Mixref, Low_x2, Low_/2, Medium_x2, Medium_/2, High_x2 and High_/2. Dunnett test applied to compare the mixtures to Mixref, considered as a control. *** $0 < p < 0.001$; ** $0.001 < p < 0.01$; * $0.01 < p < 0.05$;. $0,05< p < 0,1$; 0,1. Single column fitting image.

For both individual substrates and mixtures, bread presented the highest concentration of SEES (949.34 ± 88.21 mg/g_{VS}) and the highest H_2 production (184.63 ± 10.64 mLH_2/g_{VS}). Alibardi and Cossu (2016) reported a similar H_2 yield (167 mLH_2/g_{VS}) using a fraction of bread-pasta composed of 82 % (TS) carbohydrates (Alibardi and Cossu, 2016). On the other side, the lowest H_2 yields of 9.69 ± 1.68 mLH_2/g_{VS} and 4.25 ± 2.37 mLH_2/g_{VS} were obtained for the substrates showing the lowest sugar contents: 160.54 ± 56.58 mg/g_{VS} for rye silage and 9.85± 1.66 mg/g_{VS} for steak, respectively. Domanski *et al.* (2020) reported a similar yield of 10 mLH_2/g_{VS} with rye straw under mesophilic conditions (35 °C) and after 1-h heat pretreatment at 121°C (Domański et al., 2020). Regarding protein- and lipid-rich substrates, Alibardi and Cossu (2016) observed a yield five times lower than for the steak, with a Meat Fish Cheese fraction (yield of 0.8 mLH_2/g_{VS}) composed of 12 % TS carbohydrates, 33 % TS lipids and 52 % TS proteins (Alibardi and Cossu, 2016).

Interestingly, a positive linear correlation between H_2 yield and SEES (mg/g_{VS}) was observed for both individual substrates and mixtures (Fig. 3-A). The sugar content of the mixed vegetables was considered as an outlier, with a concentration exceeding 1000 mg/g_{VS} (i.e., 1073 mg/g_{VS}). This data point was excluded from the composition and correlations analyses (Fig. 3-A and Fig. 3-B). This high value was attributed to potential interactions with the anthrone reactant, although the interferences remain to be identified. Similarly, Juo and Stotzky (1967) observed an overestimation of absorbance (+ 40 %) when nitrate and nitrite were added to a standard glucose solution (0.1 mg/mL) up to a concentration of 0.005 mol/L (Juo and Stotzky, 1967).

The linear correlation between H_2 yield and SEES corroborated the one obtained by Guo et al. (2014) who used a similar method to measure soluble carbohydrates (acid hydrolysis step (2 M HCl) followed by anthrone dosage)(Guo et al., 2014). This method determines soluble and easily extractible sugars contents of organic substrates and does not account for all hemicellulose or cellulose content from lignocellulosic materials. This could explain the loss of information concerning the macro-composition of rye silage (Table 3). In the case of Guo et al. (2014) study, they build a predictive model of substrate BHP based on the soluble sugar content of carbohydrate-rich substrates, protein-rich substrates and lignocellulosic substrates (agri-industrial waste and agricultural end-products) with a linear regression model (R^2 = 0.89). Monlau et al. (2012) also found a strong correlation between H_2 yield (expressed in mLH_2/g_{TS}) and soluble sugars (%TS) for individual lignocellulosic substrates (composition between 0 % and 59.1 % TS of SEES and 2.3–29.7 % TS proteins) with a R^2 of 0.95 (Monlau et al., 2012). In this case, soluble sugars were obtained after mild acid hydrolysis conditions (121 °C, 1 h using 0.2 % H_2SO_4 (w/w)). Interestingly, Alibardi and Cossu (2016) observed a similar correlation between H_2 yield and carbohydrates, but in their case it concerned total carbohydrates instead of soluble sugars (Alibardi and Cossu, 2016). Fig. 3-B presents the linear correlation of H_2 yield (mLH_2/g_{TS}) with SEES (mg/g_{TS}) including the values of soluble sugars issued from Guo et al. (2014) and Monlau et al. (2012). Our study completed the previous ones (Guo et al. 2014 and Monlau et al. 2012) by including lipid-containing waste and mixtures of substrates. Fig. 3-B shows that the correlation remained relevant for the whole substrates. Therefore, the presence of lipids in our study did not seem to interfere with the soluble sugar – H_2 yield correlation. This observation was confirmed since no significant correlations were found between protein content, lipid content and H_2 yield (respectively p-value = 9.6×10^{-2} and p-value = 1.47×10^{-1}) for the entire range of substrates studied. Alibardi and Cossu (2016) observed a similar trend, where H_2 production was only correlated to carbohydrate content and not with protein nor lipid content (Alibardi

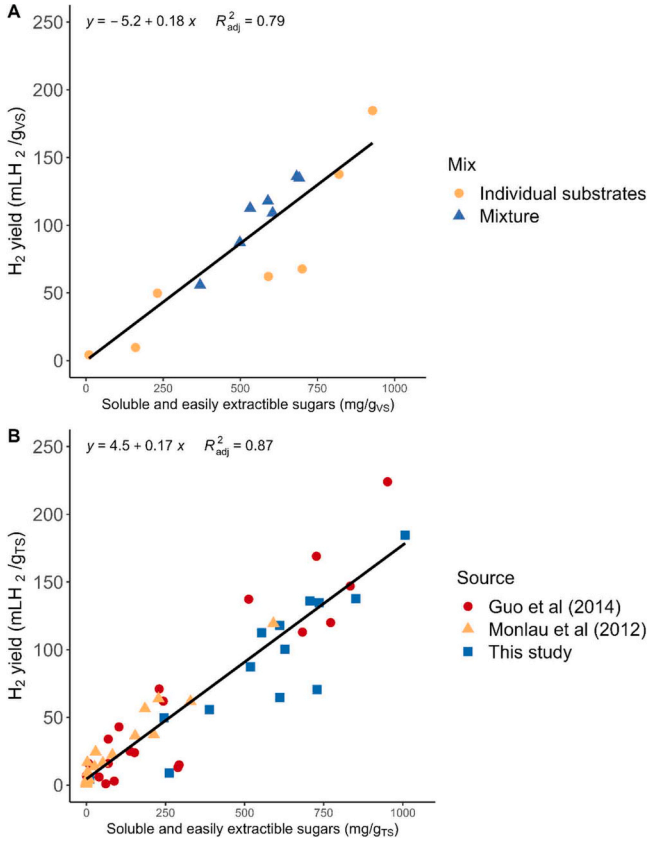

Fig. 3. Linear correlation between H_2 yield and SEES (mg/g_{VS}). 3-A: linear correlations between H_2 yield and SEES content for the individual substrates and mixtures studied. 3-B: linear correlation between H_2 yield (mL_{H2}/g_{TS}) and SEES, completed with Guo, 2012 and Monlau, 2012 (Guo, 2012; Monlau, 2012). For the correlation results the substrate Mix of vegetables was not taken into account due to its outlier sugar content. Single column fitting image.

Table 3
Conversion rate, kinetics parameters (R, maximal production rate and λ, lag phase from Gompertz modelling), and Hydrogen Production Efficiency (HPE) for individual and mixed substrates. Mean values (n=3) ± standard-deviation.

Substrates	Conversion rate (%)	R (mLH_2/g_{VS}/d)	λ (d)	HPE
Steak	18.46 ± 5.10	22.28 ± 19.15	0.47 ± 0.04	0.02 ± 0.01
Rye silage	20.67 ± 1.71	37.28 ± 12.51	0.48 ± 0.11	0.16 ± 0.05
Yogurt	35.27 ± 4.08	111.37 ± 46.08	0.50 ± 0.02	0.27 ± 0.03
Red berries	47.40 ± 1.20	137.50 ± 17.99	0.41 ± 0.02	0.45 ± 0.10
Breaded fish	60.72 ± 3.15	82.47 ± 18.25	0.71 ± 0.05	0.40 ± 0.06
Vegetables	45.26 ± 0.30	122.10 ± 17.96	0.37 ± 0.006	0.71 ± 0.02
French fries	62.53 ± 4.30	177.52 ± 47.49	0.47 ± 0.02	0.67 ± 0.10
Bread	73.88 ± 1.95	262.71 ± 11.70	0.50 ± 0.04	0.76 ± 0.02
Mixref	38.40 ± 1.35	325.21 ± 45.41	0.39 ± 0.07	0.74 ± 0.13
Low_/2	49.94 ± 2.23	321.69 ± 41.75	0.33 ± 0.04	0.76 ± 0.04
Low_x2	29.79 ± 1.14	249.00 ± 21.50	0.25 ± 0.004	0.40 ± 0.02
Medium_x2	39.22 ± 3.69	256.55 ± 58.41	0.36 ± 0.01	0.70 ± 0.11
Medium_/2	49.44 ± 0.73	361.82 ± 24.18	0.36 ± 0.03	0.64 ± 0.02
High_x2	44.86 ± 2.67	369.30 ± 12.63	0.43 ± 0.009	0.88 ± 0.08
High_/2	33.28 ± 0.89	291.16 ± 29.63	0.34 ± 0.04	0.63 ± 0.04

and Cossu, 2016) Therefore, soluble carbohydrates appeared to be the only component driving H_2 production, while proteins and lipids did not affect the production.

In addition, we confirmed that the soluble sugar- H_2 yield correlation was consistent even with the mixtures of substrates, as observed by Alibardi and Cossu (2016). In contrast some authors reported that the presence of proteins and lipids in the mixture composition could have influenced H_2 production. Tarazona et al. (2022) demonstrated that, when maintaining a fixed carbohydrate concentration of 15 g/L, a significant decrease in H_2 production (maximal production, maximal production rate and H_2 yield) was observed when the proportions of synthetic proteins (hydrolyzed casein) and lipids (virgin oil) were lower than 10 %, whereas low H_2 production was observed for lipids and proteins individually (Tarazona et al., 2022). Therefore, it appears that lipids and proteins could play an indirect role on H_2 production, but not in the present study, likely due to the different nature of lipids, proteins and microbial community composition.

3.2. Identification of positive interactions for H_2 production observed in mixed substrates

To investigate the potential interactions for H_2 production that can be observed during co-fermentation, the expected and experimental H_2 yields of the seven mixtures were compared. Fig. 4A represents both the experimental yields and expected yields estimated from those of the individual substrates (weighted sum of the individual performances of mixtures components). No significant differences were observed between the experimental and expected yields of Mixref, High_x2 and Low_x2 mixtures. The experimental yields significantly exceeded the expected ones for the mixtures High_/2, Medium_x2, Medium_/2 and Low_/2 with experimental values between 16 % and 37 % above the expected values (one sample t-test, expected values as reference, p-value < 0.03). Similar positive interactions were also observed by Tepari et al. (2020) during co-digestion of Bovine Serum Albumine (BSA) and starch at various proportions (BSA:Starch 80:20, 50:50, 20:80). In all the tested mixtures, the experimental H_2 volume exceeded the expected one by 9, 25 and 38 %, respectively (Tepari et al., 2020). Positive interactions observed in the literature during co-digestion studies were typically explained as the result of various benefits of co-digestion, including the dilution of toxic or inhibitory compounds, better pH control and stability, and optimization of the Carbohydrate/Protein (C/N) ratio (De Gioannis et al., 2013).

3.3. Substrate conversion is not favored in mixed substrates

The synergetic effect observed by mixing different substrates was

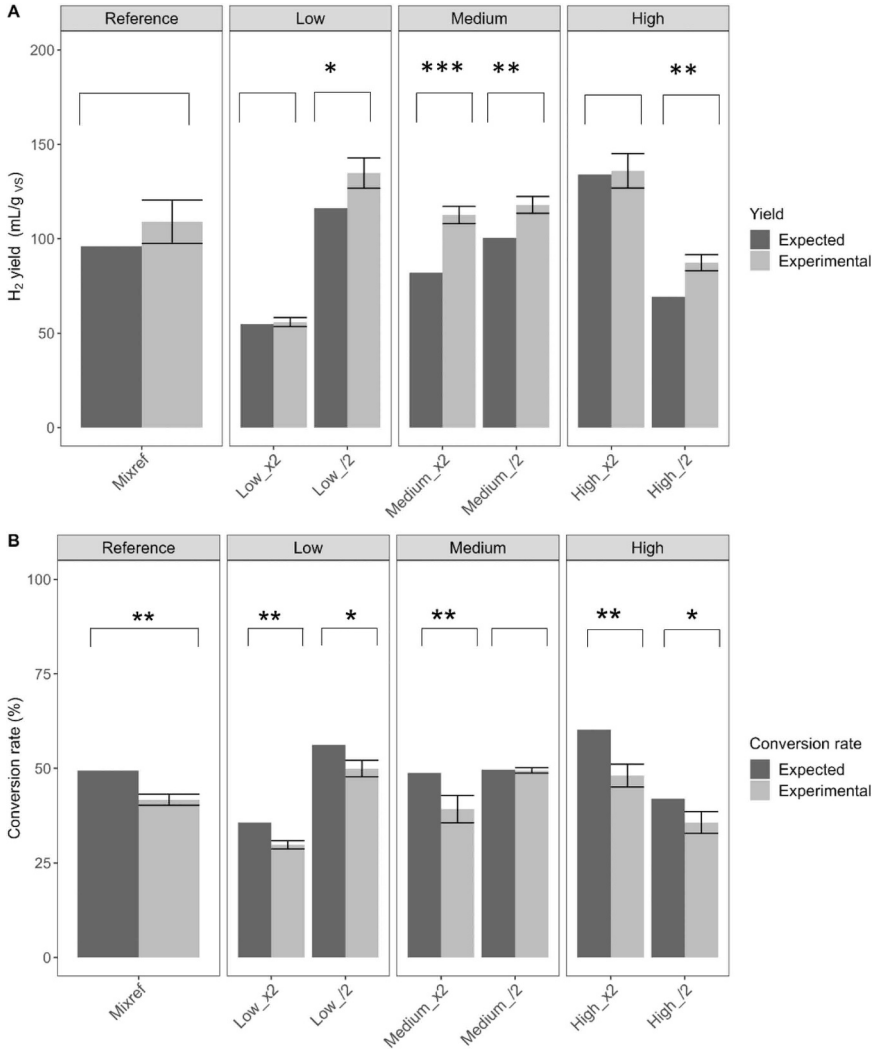

Fig. 4. Comparing the experimental and expected values for H_2 yield (mL_{H2}/g_{VS}) (Fig. 4-A) and conversion rate (%) (Fig. 4-B). Comparison between expected and experimental values were done using one sample t test and considering expected values as theoretical values. *** $0 < p < 0.001$; ** $0.001 < p < 0.01$; * $0.01 < p < 0.05$;. $0{,}05 < p < 0{,}1$; 0,1. Single column fitting image.

also studied for total substrate degradation. The total Chemical Oxygen Demand (COD) conversion was calculated based on soluble metabolites and H_2 production (*i.e.* conversion rate, Table 3) for individual substrates and mixtures, on the basis of the total biodegradable COD. For individual substrates, the highest COD conversion (74 %) was achieved for bread, while the lowest (20 %) was obtained for steak. In mixed substrates, the overall COD conversion was ranging between 29 % and 59 %.

To estimate to what extent the substrate conversion could have been improved using mixed substrate mixtures, the experimental conversion (based on experimental measurement of soluble metabolites and H_2 production) was compared with the expected one -calculated as for expected H_2 yield, with the weighted sum of each individual productions. Fig. 4-B represents the experimental and expected conversion rate for the studied mixtures. All mixtures except Medium_/2 exhibited experimental conversion rates significantly lower than the expected values (one sample t-test with expected values considered as reference, p-values < 0.02). Therefore, substrate hydrolysis was not improved with the mixtures and cannot be related to the enhanced H_2 production observed in mixtures. On the contrary, Yang et al. (2019) observed an improved substrate degradation with a higher VS removal for the mixture 20:20 (sewage sludge:fallen leaves) compared to their respective mono-fermentations (Yang et al., 2019). In this study, the lower COD conversion observed with mixtures could be explained by the mutual presence of carbohydrates, lipids and proteins, affecting their overall degradation. Indeed, while carbohydrate-rich substrates are more favorable for their conversion into H_2 and VFA, protein and lipid-rich substrates present challenges to be degraded due to thermodynamic inhibitions. In addition, Tepari et al. (2020) showed that particulate carbohydrates had a negative impact on particulate proteins degradation rate during the co-digestion of starch and BSA (Tepari et al., 2020). The authors explained this phenomenon by the more readily biodegradable nature of starch compared to proteins and the potential repression of protease formation by glucose (Breure et al., 1986; Tepari et al., 2020).

3.4. H_2 production was faster with mixed substrates

Kinetic parameters were compared between individual substrates and their mixtures (Table 3). The results showed that the maximal production rate (R) of these mixtures significantly exceeded the individual substrates (Wilcoxon test, p-value $= 6.67\times10^{-13}$). The maximal hydrogen production rate of the mixtures ranged from 249 to 361 $mLH_2/g_{VS}/d$, while it ranged from 22 to 263 $mLH_2/g_{VS}/d$ for individual substrates. Similarly, the lag phase (λ) was significantly lower with mixtures than individual substrates (Wilcoxon test, p-value $= 6.80\times10^{-8}$). The lag phase ranged from 0.25 to 0.43 day for the mixtures and from 0.37 to 0.71 day for individual substrates. Therefore, hydrogen production was accelerated for mixtures, with less variability of the kinetics parameters.

Contrary to the H_2 yield, H_2 maximal production rate did not show a strong correlation with the SEES content (Pearson correlation $= +0.433$, p-value $= 3.34\times10^{-2}$). Thus, H_2 production rate was likely influenced by the whole composition of the substrates rather than only carbohydrates. Indeed, proteins and lipids are also impacting the bacterial physiology (Tarazona et al., 2022). In particular, amino acids from proteins hydrolysis can be used by the cells to stimulate microbial growth, leading to an improved H_2 production and productivity (Sharma and Melkania, 2018). Sharma and Melkania (2018) showed that a supplementation in amino acids (methionine, alanine, histidine, cysteine and lysine) improved H_2 production from the organic fraction of municipal solid waste in a co-culture of *Escherichia coli* and *Enterobacter aerogenes* (Sharma and Melkania, 2018). A well-balanced composition of carbohydrates and proteins in the studied mixtures can likely favor bacterial growth, resulting in shorter adaptation phase (i.e., lag phase) and faster H_2 production rate, causing the observed positive interactions.

3.5. Metabolites production and metabolic pathways

The lower H_2 production rate observed with individual substrates could also be attributed to the development of competitive pathways or H_2-consuming pathways. To confirm this hypothesis, the profiles of soluble metabolites at the end of H_2 production were compared for the different substrates. The main soluble metabolites produced were butyrate and acetate in all conditions (supplementary file S2). The final concentration of butyrate strongly correlated with the H_2 yield (Pearson correlation $= +0.858$, p-value $= 8.52\times10^{-5}$) and to SEES concentration (Pearson correlation $= +0.649$, p-value $= 1.05\times10^{-3}$). In contrast, the acetate concentration did not significantly correlate with the H_2 yield (p-value $= 2.46\times10^{-1}$) nor the SEES content (p-value $= 1.99\times10^{-1}$). This is consistent with Guo et al. (2014) who observed that the accumulation of butyrate was strongly related to H_2 production and not acetate: Indeed, butyrate production was specifically linked to H_2 producing pathways through the butyrate pathway (Eq. 1). Meanwhile acetate could be related to H_2 release through the acetate pathway (Eq. 2), but other pathways related to acetate accumulation can also occur, such as homoacetogenesis (Eq. 5) (Guo et al., 2014).

$$C_6H_{12}O_6 \rightarrow CH_3CH_2CH_2COOH + 2CO_2 + 2H_2 \quad (3)$$

$$C_6H_{12}O_6 + 2\ H_2O \rightarrow 2CH_3COOH + 2CO_2 + 4H_2 \quad (4)$$

$$4H_2 + 2CO_2 \rightarrow CH_3COOH + 2H_2O \quad (5)$$

Interestingly, acetate production with almost no H_2 was observed with the steak substrate (4 mL_{H2}/g_{VS}). This acetate production could come from the degradation of proteins via the Stickland pathway, corresponding to a coupled deamination of two amino acids such as alanine and glycine (Eq. 6)(Nisman, 1954).

$$CH_3CH(COOH)NH_2 + 2H_2O + 2CH_2(COOH)NH_2 \rightarrow 3CH_3COOH + CO_2 + 3NH_3 \quad (6)$$

Regarding the low concentrations of other metabolites, it appears that no major competitive pathways (lactate, alcohols…) were predominantly followed over H_2 production for either individual substrates or mixtures. However, in the mixture of substrates, the profile of soluble metabolites appeared to be less diverse regarding the minor metabolites (supplementary file S2), suggesting that mixed substrates could redirect carbon fluxes towards acetate and butyrate pathways with less minor competitive pathways followed.

3.6. Reduced H_2-consumption by homoacetogens in mixed substrates

Since no major differences in the metabolic pathways was observed between individual and mixed substrates, the apparent slower H_2 production in individual substrates was probably due to the consumption of H_2 by homoacetogenic bacteria through homoacetogenesis (Eq. 5). To confirm this hypothesis, a Hydrogen Production Efficiency (HPE) index was calculated for all the tested conditions (Table 3). An index of 1 indicates that acetate is produced only through the acetate pathway (i.e.,

related to H_2 production). An index lower than 1 suggests that part of acetate is produced by homoacetogenesis. The HPE of individual substrates ranged from 0.02 to 0.76 and the HPE of mixtures ranged from 0.40 to 0.88. As HPE was always lower than 1 for all the substrates, this indicated that H_2 was partly consumed by homoacetogens in all conditions. In addition, the HPE was significantly higher for the mixtures than individual substrates (Wilcoxon test, p-value $= 3.06\times10^{-4}$), with values closer to 1. For instance, French fries presented an HPE of 0.67, compared to 0.75 for Low_/2 and 0.88 for High_x2, all with similar H_2 yields (respectively 137.65, 134.78 and 135.93 mLH_2/g_{VS}). According to HPE comparison, H_2 consumption via homoacetogenesis was higher for individual substrates, leading to a lower apparent H_2 production compared to the mixtures.

In addition, the growth of microbial community was monitored during the fermentation stage. qPCR analyses were performed to quantify total bacteria, Hydrogen-Producing Bacteria (HPB) and homoacetogens. Fig. 5 presents the growth of total bacteria, HPB and homoacetogens from initial to final samplings for each substrate. No significant differences were observed between individual substrates and mixtures in terms of total bacteria growth (Wilcoxon test, p-value $= 4.25\times10^{-1}$). However, the growth of hydrogen-producing bacteria was significantly higher in mixtures (Wilcoxon test, p-value $= 2.26\times10^{-3}$). This result aligns with the increased H_2 production rate and the synergy observed with mixed substrates. Therefore, using mixtures was always more favorable to the growth of HPB.

Regarding the homoacetogenic bacteria, no growth was observed in the mixtures. However, a significant difference between mixture and individual substrates was observed (Wilcoxon test, p-value $=3.41\times10^{-4}$). The growth of HPB was therefore favored at the expense of homoacetogenic bacteria with mixed substrates.

3.7. Microbial communities

Differences in growth between HPB and homoacetogenic bacteria suggested distinct microbial communities between individual and mixed substrates. Fig. 6 shows the relative abundances of the major bacterial families in mixtures and individual substrates at the end of fermentation. In mixtures, members of the *Clostridiaceae_1* family were mostly favored, with relative abundances ranging between 90 % and 98 %. In particular, the *Clostridium_sensus_stricto_1* genus was the main genus observed in mixtures, excepting for the High_x2 mixture where *Clostridium_sensus_stricto_5* was the major genus (supplementary file S3). For individual substrates, the composition in families was more diversified, including *Clostridiaceae_1* (7 – 81 %), *Enterobacteriaceae* (6–70 %), *Streptococcaceae (0.05 % –50 %)* and *Enterococcaceae (0.05 % –10 %)* families detected. The *Clostridiaceae_1* family and in particular the *Clostridium* genus, are rod-shaped bacteria, obligate anaerobes and are well-known to produce H_2 (Vos et al., 2011). *Enterococcaceae* and *Enterobacteriaceae* are facultative anaerobic fermentative bacteria that can also produce hydrogen (Rosenberg et al., 2014). Nonetheless, lactic acid bacteria can also be found in the *Enterobacteriaceae* and *Streptococcaceae* families (Palomo-Briones et al., 2017). The role of Lactic Acid Bacteria (LAB) in DF remains unclear since negative interactions have been observed between LAB and HPB (substrate competition, bacteriocins production)(Palomo-Briones et al., 2017), but also positive interactions were previously suspected (lactose fermentation, lactate conversion to butyrate) (Castelló et al. 2020). Here, no lactate was detected at the end of fermentation for the whole substrates studied suggesting that LAB were not present or lactate was immediately consumed to produce butyrate and H_2.

In individual substrate fermentation, *Clostridiaceae_1* was the main family for bread, French fries (respective relative abundance of 81 and 66 %). For these two substrates, the most abundant genus was *Clostridium sensu stricto 5* (supplementary file S3). Surprisingly, for the steak fermentation 72 % of the final microbial community was composed of *Clostridiaceae_1*. As it was previously suggested with the metabolites results, the Stickland reaction was probably carried out by members of the *Clostridiaceae* family (in particular the *Clostridiaceae_1_unclassified* genus; supplementary file S3) explaining the low H_2 production obtained for this substrate and the high abundance in *Clostridiaceae*. Most of the species in this family have the capacity to degrade amino acids by coupled deamination (Nisman, 1954; Nagase and Matsuo, 1982). Similar results were observed by Yang and Wang (2021), where co-fermentation of antibiotic fermentation residues and fallen leaves resulted in an enrichment of the *Clostridium sensu stricto 1* genus at 93.6 % at the end of fermentation, compared to 27.1 and 89.1 % for the respective mono-fermentation of each substrate (Yang and Wang, 2021). Besides, they observed a higher dehydrogenase activity and enrichment of hydrogen-producing functional genes resulting in a synergy for H_2 production in co-fermentation (Yang and Wang, 2021).

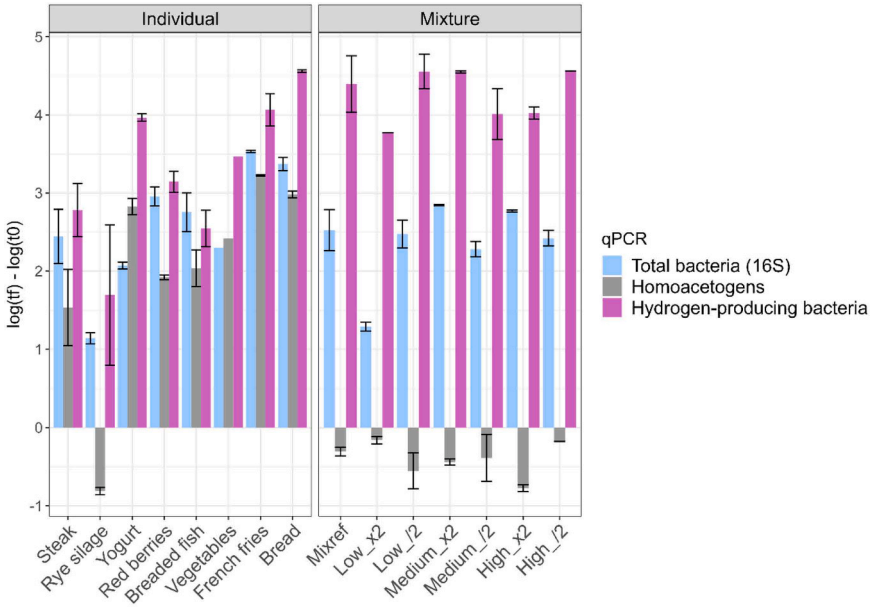

Fig. 5. Growth of total bacteria, homoacetogens and hydrogen-producing bacteria based on qPCR analyses. Growth is estimated by the difference between final and initial sample for a given substrate. Duplicates were analyzed for final samples, except for vegetables. Single column fitting image.

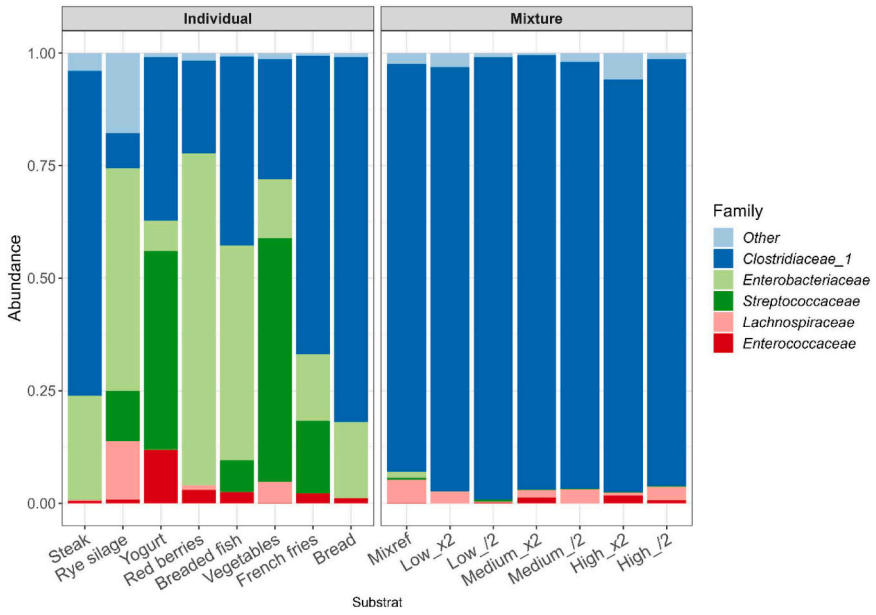

Fig. 6. The relative abundance of the five most abundant families for the final samples for individual substrates and mixtures. Single column fitting image.

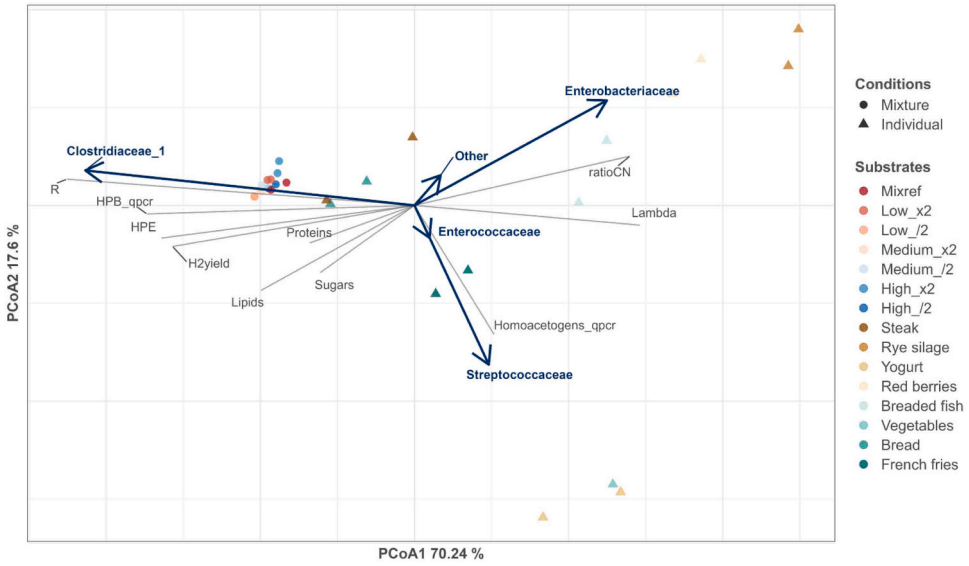

Fig. 7. PcoA with major families represented with bold blue arrows and environmental variables (grey arrows): H_2 yield ("H2yield"), maximal production rate (R), lag phase (Lambda), qPCR results for hydrogen-producing bacteria (HPB_qpcr), qPCR results for homoacetogenic bacteria (Homoacetogens_qpcr), Hydrogen Production Efficiency (HPE), C/N ratio (CN_ratio), SEES concentration (sugars), protein concentration (proteins) and lipid concentration (lipids) were fitted on the ordination plot (grey arrows) using envfit function. 2-column fitting image.

A PCoA was performed to compare the structure of the microbial communities between final samples at family level (Fig. 7). The mixtures and individual substrates are separated along the first axis, according to the H_2 production rate (70 % of the variance). Families with the strongest covariance to the microbial community variation are represented with bold blue arrows on the PCoA plot. *Clostridiaceae_1* correlates strongly with the PCoA1 axis. As observed in Fig. 6, the main difference between mixtures and individual substrates is the dominance of *Clostridiaceae_1* in the mixtures and a higher microbial diversity in individual substrates. Therefore, the composition of the substrates impacted the final microbial community, even though the same inoculum was initially used. Rocha et al. (2023) noted that the co-fermentation of citrus peel waste and citrus processing wastewater resulted in a lower diversity and higher microbial dominance (Shannon and Simpson indices) in co-fermentation conditions (Rocha et al., 2023).

Environmental variables were overlaid on the PCoA plot using envfit function to get a global overview and show which factors could have impacted the community structure. The longer the arrows are, the stronger the correlations are between the variable and the principal components of the ordination plot. Details of the envfit function results are given in supplementary file S4.

The maximum H_2 production rate (R) was the variable correlating the most with *Clostridiaceae_1* relative abundance. A positive linear correlation was indeed found between *Clostridiaceae_1* relative abundance and the maximal production rate, R (Fig. 8, Pearson correlation = $+0.909$, p-value = 3.13×10^{-4}). Interestingly, *Enterobacteriaceae* relative abundance negatively correlated with R (Fig. 8, Pearson correlation = -0.749, p-value = 6.32×10^{-3}). Therefore, *Clostridiaceae_1* abundance was

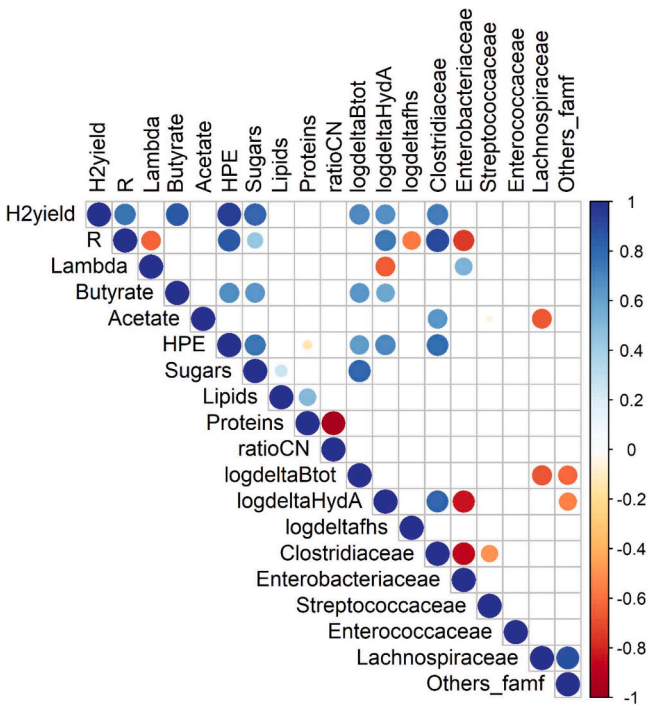

Fig. 8. Pearson correlation matrix for mixtures and individual substrates for the following variables: H_2 yield ("H2yield"), maximal H_2 production rate ("R"), lag phase ("Lambda"), conversion rate ("advancement"),Hydrogen Production Efficiency ("HPE"), SEES concentration ("sugars"), protein concentration ("proteins"), lipid concentration ("lipids"), C/N ratio ("ratioCN"), growth of total bacteria, hydrogen-producing bacteria and homoacetogen bacteria according to qPCR results (respectively "logdeltaBtot","logdeltaHydA","-logdeltaFHS") and final relative abundance at family level ("Clostridiaceae", "Enterobacteriaceae", "Streptococcaceae", "Enterococcaceae", "Lachnospiraceae", "Others_famf"). Only significant correlations (p-value < 0.05) are displayed. Single column fitting image.

one of the factor explaining the highest H_2 production rate observed with the mixtures of substrate. Additionally, the growth of *Enterobacteriaceae* family in individual substrates could explain the slower H_2 production observed. Regarding the homoacetogenic bacteria, members of the *Streptococcaceae* family could be related to the growth of homoacetogenic bacteria ("Homoacetogens_qpcr") according to Fig. 7. A correlation of 0.648 was indeed observed and was close to be significant (p-value = 0.071, data not shown). However, no significant correlation was found between homoacetogens growth and substrate composition (Fig. 7, Fig. 8).

4. Conclusion

In this study, the impact of the composition (sugars, lipids and proteins) of individual substrates and mixtures conditions on dark fermentation performances was investigated. A linear correlation between the H_2 yield and the SEES content was observed for both individual and substrate mixtures. Moreover, positive interactions were observed with mixed substrates, with H_2 yields significantly higher than expected. Based on kinetics modeling and microbial community analyses, it was concluded that mixtures favored the growth of a specific family of HPB (*Clostriadiaceae_1*) at the expense of homoacetogenic bacteria. Further investigations are needed to understand the favored growth of *Clostridiaceae_1* in mixtures. In addition, the decline of homoacetogenic bacteria in mixtures needs to be confirmed and further examine in complementary studies. A better understanding of H_2-producing and H_2-consuming bacteria dynamics in dark co-fermentation would help to valorize complex waste stream with a better control and stability. This preliminary study provides insight for DF-AD coupling by identifying which substrates or co-substrates can be favored in DF step, based on their soluble carbohydrate content. An integrative study would be interesting to observe the impact of co-fermentation on the successive stages of DF and AD and global energy recovery.

Charlotte Richard:Conceptualization, Supervision, Validation, Writing – review & editing. **Nicolas Bernet**:Conceptualization, Supervision, Validation, Writing – review & editing. **Marine Juge**:Conceptualization, Funding acquisition, Supervision, Validation, Writing – review & editing. **Mathilde Jégoux**:Supervision, Validation. **Renaud Escudié**:Conceptualization, Supervision, Validation, Writing – review & editing. **Lucie Perat**:Conceptualization, Formal analysis, Investigation, Visualization, Writing – original draft, Writing – review & editing. **Eric Trably**:Conceptualization, Funding acquisition, Supervision, Validation, Writing – review & editing

Declaration of Competing Interest

The authors declare that they have no known competing financial interests or personal relationships that could have appeared to influence the work reported in this paper.

Acknowledgments

The research was funded by the Occitanie region and ENGIE Lab CRIGEN, with grant number UFTMIP 2021 521-CIF-D-DRDV Défi clé Hydrogen Vert - MELINBIOH. The authors would like to thank Gaëlle Santa-Catalina for performing the biomolecular analyses. The authors would like also to thank INRAE Bio2E Facility (Bio2E, INRAE, 2018. Environmental Biotechnology and Biorefiney Facility (https://doi.org/10.15454/1.557234103446854E12) where some of the experiments were conducted.

Appendix A. Supporting information

Supplementary data associated with this article can be found in the online version at doi:10.1016/j.psep.2024.06.006.

References

ADEME (2021) Prospective - Transitions 2050 - Rapport No 011627. In: La librairie ADEME. https://librairie.ademe.fr/recherche-et-innovation/5072-prospective-transitions-2050-rapport.html. Accessed 10 May 2024.

Alibardi, L., Cossu, R., 2015. Composition variability of the organic fraction of municipal solid waste and effects on hydrogen and methane production potentials. Waste Manag. 36, 147–155. https://doi.org/10.1016/j.wasman.2014.11.019.

Alibardi, L., Cossu, R., 2016. Effects of carbohydrate, protein and lipid content of organic waste on hydrogen production and fermentation products. Waste Manag. 47, 69–77. https://doi.org/10.1016/j.wasman.2015.07.049.

Arooj, M., Han, S., Kim, S., et al., 2008. Continuous biohydrogen production in a CSTR using starch as a substrate. Int. J. Hydrog. Energy 33, 3289–3294. https://doi.org/10.1016/j.ijhydene.2008.04.022.

Ben Yahmed, N., Dauptain, K., Lajnef, I., et al., 2021. New sustainable bioconversion concept of date by-products (Phoenix dactylifera L.) to biohydrogen, biogas and date-syrup. Int. J. Hydrog. Energy 46, 297–305. https://doi.org/10.1016/j.ijhydene.2020.09.203.

Boni, M.R., Sbaffoni, S., Tuccinardi, L., 2013. The influence of slaughterhouse waste on fermentative H2 production from food waste: preliminary results. Waste Manag. 33, 1362–1371. https://doi.org/10.1016/j.wasman.2013.02.024.

Braga Nan, L., Trably, E., Santa-Catalina, G., et al., 2020. Biomethanation processes: new insights on the effect of a high H2 partial pressure on microbial communities. Biotechnol. Biofuels 13, 141. https://doi.org/10.1186/s13068-020-01776-y.

Breure, A.M., Mooijman, K.A., van Andel, J.G., 1986. Protein degradation in anaerobic digestion: influence of volatile fatty acids and carbohydrates on hydrolysis and acidogenic fermentation of gelatin. Appl. Microbiol. Biotechnol. 24, 426–431. https://doi.org/10.1007/BF00294602.

Bundhoo, M.A.Z., Mohee, R., 2016. Inhibition of dark fermentative bio-hydrogen production: a review. Int. J. Hydrog. Energy 41, 6713–6733. https://doi.org/10.1016/j.ijhydene.2016.03.057.

Castelló, E., Nunes Ferraz-Junior, A.D., Andreani, C., et al., 2020. Stability problems in the hydrogen production by dark fermentation: possible causes and solutions.

Renew. Sustain. Energy Rev. 119, 109602 https://doi.org/10.1016/j.rser.2019.109602.
Charnier, C., Latrille, E., Jimenez, J., et al., 2017. Fast characterization of solid organic waste content with near infrared spectroscopy in anaerobic digestion. Waste Manag. 59, 140–148. https://doi.org/10.1016/j.wasman.2016.10.029.
Chatellard L. (2016) Production of biological hydrogen by dark fermentation of lignocellulosic residues: Links between substrate composition and structure of fermentative microbial communities. Phdthesis, Institut National d'Etudes Supérieures Agronomiques de Montpellier.
Chen, Y., Yin, Y., Wang, J., 2021. Recent advance in inhibition of dark fermentative hydrogen production. Int. J. Hydrog. Energy 46, 5053–5073. https://doi.org/10.1016/j.ijhydene.2020.11.096.
Cremonez, P.A., Teleken, J.G., Weiser Meier, T.R., Alves, H.J., 2021. Two-Stage anaerobic digestion in agroindustrial waste treatment: a review. J. Environ. Manag. 281, 111854 https://doi.org/10.1016/j.jenvman.2020.111854.
Dauptain, K., Schneider, A., Noguer, M., et al., 2021. Impact of microbial inoculum storage on dark fermentative H2 production. Bioresour. Technol. 319, 124234 https://doi.org/10.1016/j.biortech.2020.124234.
Dauptain, K., Trably, E., Santa-Catalina, G., et al., 2020. Role of indigenous bacteria in dark fermentation of organic substrates. Bioresour. Technol. 313, 123665 https://doi.org/10.1016/j.biortech.2020.123665.
De Gioannis, G., Muntoni, A., Polettini, A., Pomi, R., 2013. A review of dark fermentative hydrogen production from biodegradable municipal waste fractions. Waste Manag. 33, 1345–1361. https://doi.org/10.1016/j.wasman.2013.02.019.
Dincer, I., Acar, C., 2015. Review and evaluation of hydrogen production methods for better sustainability. Int. J. Hydrog. Energy 40, 11094–11111. https://doi.org/10.1016/j.ijhydene.2014.12.035.
Domański, J., Marchut-Mikołajczyk, O., Cieciura-Włoch, W., et al., 2020. Production of Methane, Hydrogen and Ethanol from Secale cereale L. Straw Pretreated with Sulfuric Acid. Molecules 25, 1013. https://doi.org/10.3390/molecules25041013.
Dong, L., Zhenhong, Y., Yongming, S., et al., 2009. Hydrogen production characteristics of the organic fraction of municipal solid wastes by anaerobic mixed culture fermentation. Int. J. Hydrog. Energy 34, 812–820. https://doi.org/10.1016/j.ijhydene.2008.11.031.
Ghimire, A., Frunzo, L., Pontoni, L., et al., 2015. Dark fermentation of complex waste biomass for biohydrogen production by pretreated thermophilic anaerobic digestate. J. Environ. Manag. 152, 43–48. https://doi.org/10.1016/j.jenvman.2014.12.049.
Gomez-Romero, J., Gonzalez-Garcia, A., Chairez, I., et al., 2014. Selective adaptation of an anaerobic microbial community: biohydrogen production by co-digestion of cheese whey and vegetables fruit waste. Int. J. Hydrog. Energy 39, 12541–12550. https://doi.org/10.1016/j.ijhydene.2014.06.050.
Guo X. (2012) Biohydrogen Production and Metabolic Pathways in Dark Fermentation Related to the Composition of Organic Solid Waste. Theses, Université Montpellier 2 (Sciences et Techniques).
Guo, X., Trably, E., Latrille, E., et al., 2014. Predictive and explicative models of fermentative hydrogen production from solid organic waste: role of butyrate and lactate pathways. Int. J. Hydrog. Energy 39, 7476–7485. https://doi.org/10.1016/j.ijhydene.2013.08.079.
Hanaki, K., Matsuo, T., Nagase, M., 1981. Mechanism of inhibition caused by long-chain fatty acids in anaerobic digestion process. Biotechnol. Bioeng. 23, 1591–1610. https://doi.org/10.1002/bit.260230717.
Henderson, C., 1973. The effects of fatty acids on pure cultures of rumen bacteria. J. Agric. Sci. 81, 107–112. https://doi.org/10.1017/S0021859600058378.
International Energy Agency (2021) Global Hydrogen Review 2021. OECD.
Juo, P.S., Stotzky, G., 1967. Interference by nitrate and nitrite in the determination of carbohydrates by anthrone. Anal. Biochem. 21, 149–151.
Kahm, M., Hasenbrink, G., Lichtenberg-Frate, H., et al., 2010. Grofit: fitting biological growth curves. Nat. Preced. https://doi.org/10.1038/npre.2010.4508.1.
Lay, J.-J., Fan, K.-S., Chang, J.-1, Ku, C.-H., 2003. Influence of chemical nature of organic wastes on their conversion to hydrogen by heat-shock digested sludge. Int. J. Hydrog. Energy 28, 1361–1367. https://doi.org/10.1016/S0360-3199(03)00027-2.
Luo, G., Karakashev, D., Xie, L., et al., 2011. Long-term effect of inoculum pretreatment on fermentative hydrogen production by repeated batch cultivations: homoacetogenesis and methanogenesis as competitors to hydrogen production. Biotechnol. Bioeng. 108, 1816–1827. https://doi.org/10.1002/bit.23122.
Magdalena, J.A., Pérez-Bernal, M.F., Bernet, N., Trably, E., 2023. Sequential dark fermentation and microbial electrolysis cells for hydrogen production: Volatile fatty acids influence and energy considerations. Bioresour. Technol. 374, 128803 https://doi.org/10.1016/j.biortech.2023.128803.
Mariotti, F., Tomé, D., Mirand, P.P., 2008. Converting nitrogen into protein—beyond 6.25 and Jones' factors. Crit. Rev. Food Sci. Nutr. 48, 177–184. https://doi.org/10.1080/10408390701279749.
Monlau F. (2012) Application of Pretreatments to Enhance Biohydrogen And/or Biomethane from Lignocellulosic Residues: Linking Performances to Compositional and Structural Features. These de doctorat, Montpellier 2.
Monlau, F., Sambusiti, C., Barakat, A., et al., 2012. Predictive models of biohydrogen and biomethane production based on the compositional and structural features of lignocellulosic materials. Environ. Sci. Technol. 46, 12217–12225. https://doi.org/10.1021/es303132t.
Nagase, M., Matsuo, T., 1982. Interactions between amino-acid-degrading bacteria and methanogenic bacteria in anaerobic digestion. Biotechnol. Bioeng. 24, 2227–2239. https://doi.org/10.1002/bit.260241009.
Nisman, B., 1954. The Stickland reaction. Bacteriol. Rev. 18, 16–42. https://doi.org/10.1128/br.18.1.16-42.1954.
Noguer, M.C., Escudié, R., Bernet, N., Eric, T., 2022. Populational and metabolic shifts induced by acetate, butyrate and lactate in dark fermentation. Int. J. Hydrog. Energy 47, 28385–28398. https://doi.org/10.1016/j.ijhydene.2022.06.163.
Official Journal of the European Union (2011) Commission Regulation (EU) No 142/2011 of 25 February 2011 implementing Regulation (EC) No 1069/2009 of the European Parliament and of the Council laying down health rules as regards animal by-products and derived products not intended for human consumption and implementing Council Directive 97/78/EC as regards certain samples and items exempt from veterinary checks at the border under that Directive Text with EEA relevance.
Okamoto, M., Miyahara, T., Mizuno, O., Noike, T., 2000. Biological hydrogen potential of materials characteristic of the organic fraction of municipal solid wastes. Water Sci. Technol. 41, 25–32.
Oksanen, J., Blanchet, F.G., Kindt, R., et al., 2012. vegan. Community Ecol. Package.
Palomo-Briones, R., Razo-Flores, E., Bernet, N., Trably, E., 2017. Dark-fermentative biohydrogen pathways and microbial networks in continuous stirred tank reactors: novel insights on their control. Appl. Energy 198, 77–87. https://doi.org/10.1016/j.apenergy.2017.04.051.
Paradis, E., Claude, J., Strimmer, K., 2004. APE: analyses of phylogenetics and evolution in R language. Bioinformatics 20, 289–290. https://doi.org/10.1093/bioinformatics/btg412.
Policastro, G., Lamboglia, R., Fabbricino, M., Pirozzi, F., 2022. Enhancing dark fermentative hydrogen production from problematic substrates via the co-fermentation strategy. Fermentation 8, 706. https://doi.org/10.3390/fermentation8120706.
Quéméneur, M., Hamelin, J., Latrille, E., et al., 2011. Functional versus phylogenetic fingerprint analyses for monitoring hydrogen-producing bacterial populations in dark fermentation cultures. Int. J. Hydrog. Energy 36, 3870–3879. https://doi.org/10.1016/j.ijhydene.2010.12.100.
Rocha, D.H.D., Sakamoto, I.K., Varesche, M.B.A., 2023. Optimization of fermentative parameters to improve hydrogen production: is the co-fermentation of waste from the citrus agroindustrial an interesting alternative for energy recovery? J. Environ. Chem. Eng. 11, 111252 https://doi.org/10.1016/j.jece.2023.111252.
Rosenberg E., DeLong E.F., Lory S., et al (2014) The Prokaryotes: Firmicutes and Tenericutes, 4th ed. 2014 édition. Springer-Verlag Berlin and Heidelberg GmbH & Co. K, Berlin Heidelberg.
Sharma, P., Melkania, U., 2018. Enhancement effect of amino acids on hydrogen production from organic fraction of municipal solid waste using co-culture of Escherichia coli and Enterobacter aerogenes. Energy Convers. Manag. 163, 260–267. https://doi.org/10.1016/j.enconman.2018.02.072.
Shetty S., Lahti L. (2022) microbiomeutilities: microbiomeutilities: Utilities for Microbiome Analytics.
Tarazona, Y., Vargas, A., Quijano, G., Moreno-Andrade, I., 2022. Influence of the initial proportion of carbohydrates, proteins, and lipids on biohydrogen production by dark fermentation: a multi-response optimization approach. Int. J. Hydrog. Energy 47, 30128–30139. https://doi.org/10.1016/j.ijhydene.2022.01.193.
Tepari, E.A., Nakhla, G., Haroun, B.M., Hafez, H., 2020. Co-fermentation of carbohydrates and proteins for biohydrogen production: statistical optimization using Response Surface Methodology. Int. J. Hydrog. Energy 45, 2640–2654. https://doi.org/10.1016/j.ijhydene.2019.11.160.
Vos P., Garrity G., Jones D., et al (2011) Bergey's Manual of Systematic Bacteriology: Volume 3: The Firmicutes. Springer Science & Business Media.
Wang, W., Xie, L., Luo, G., Zhou, Q., 2013. Enhanced fermentative hydrogen production from cassava stillage by co-digestion: the effects of different co-substrates. Int. J. Hydrog. Energy 38, 6980–6988. https://doi.org/10.1016/j.ijhydene.2013.04.004.
Wang, J., Yin, Y., 2019. Progress in microbiology for fermentative hydrogen production from organic wastes. Crit. Rev. Environ. Sci. Technol. 49, 825–865. https://doi.org/10.1080/10643389.2018.1487226.
Wéry, N., Bru-Adan, V., Minervini, C., et al., 2008. Dynamics of Legionella spp. and bacterial populations during the proliferation of L. pneumophila in a cooling tower facility. Appl. Environ. Microbiol. 74, 3030–3037. https://doi.org/10.1128/AEM.02760-07.
Xue, S., Wang, Y., Lyu, X., et al., 2020. Interactive effects of carbohydrate, lipid, protein composition and carbon/nitrogen ratio on biogas production of different food wastes. Bioresour. Technol. 312, 123566 https://doi.org/10.1016/j.biortech.2020.123566.
Yang, G., Hu, Y., Wang, J., 2019. Biohydrogen production from co-fermentation of fallen leaves and sewage sludge. Bioresour. Technol. 285, 121342 https://doi.org/10.1016/j.biortech.2019.121342.
Yang, G., Wang, J., 2017. Co-fermentation of sewage sludge with ryegrass for enhancing hydrogen production: performance evaluation and kinetic analysis. Bioresour. Technol. 243, 1027–1036. https://doi.org/10.1016/j.biortech.2017.07.087.
Yang, G., Wang, J., 2018. Synergistic biohydrogen production from flower wastes and sewage sludge. Energy Fuels 32, 6879–6886. https://doi.org/10.1021/acs.energyfuels.8b01122.
Yang, G., Wang, J., 2021. Biohydrogen production by co-fermentation of antibiotic fermentation residue and fallen leaves: insights into the microbial community and functional genes. Bioresour. Technol. 337, 125380 https://doi.org/10.1016/j.biortech.2021.125380.
Yilmazel, Y.D., Duran, M., 2021. Biohydrogen production from cattle manure and its mixtures with renewable feedstock by hyperthermophilic Caldicellulosiruptor bescii. J. Clean. Prod. 292, 125969 https://doi.org/10.1016/j.jclepro.2021.125969.